DISTRIBUTION STATEMENT A. Approved for public release; distribution is unlimited.

DARLA: Data Assimilation and Remote Sensing for Littoral Applications

Andrew T. Jessup
Chris Chickadel, Gordon Farquharson, Jim Thomson
Applied Physics Laboratory, University of Washington
Seattle, WA 98105
phone: ((206) 685-2609 fax: (206) 543-6785 email: jessup@apl.washington.edu

Robert A. Holman
Merrick Haller, Alexander Kuropov, Tuba Ozkan-Haller
Oregon State University
Corvallis, OR 97331
phone: (541) 737-2914 fax: (541) 737-2064 email: holman@coas.oregonstate.edu

Steve Elgar
Britt Raubenheimer
Woods Hole Oceanographic Institution, MS11
Woods Hole, MA 02543
phone: (508) 289-3614 fax: (508) 457-2194 email: elgar@whoi.edu

Award Number: N000141010932

LONG-TERM GOALS

Our long-term goal is to use remote sensing observations to constrain a data assimilation model of wave and circulation dynamics in an area characterized by a river mouth or tidal inlet and surrounding beaches. As a result of this activity, we will improve environmental parameter estimation via remote sensing fusion, determine the success of using remote sensing data to drive DA models, and produce a dynamically consistent representation of the wave, circulation, and bathymetry fields in complex environments.

OBJECTIVES

The objectives are to test the following three hypotheses:

1. Environmental parameter estimation using remote sensing techniques can be significantly improved by fusion of multiple sensor products.
2. Data assimilation models can be adequately constrained (i.e., forced or guided) with environmental parameters derived from remote sensing measurements.
3. Bathymetry on open beaches, river mouths, and at tidal inlets can be inferred from a combination of remotely-sensed parameters and data assimilation models.

APPROACH

Our overall approach is to conduct a series of field experiments combining remote sensing and in situ measurements to investigate signature physics and to gather data for developing and testing DA models. To ensure early and ongoing testing, we performed a pilot experiment at Duck, NC, using tower-based remote sensing (EO, radar, IR) and current versions of the DA modeling system. We participated in the field experiments in May 2012 at New River Inlet near Camp LeJeune, NC and in May and June of 2013 at the mouth of the Columbia River near Astoria, OR under the ONR-sponsored Inlets and Rivers Mouth Dynamics Departmental Research Initiative (RIVET I and II). During this campaign, APL-UW scientist Craig McNeil and Andrea Shcherbina deployed a REMUS UUV to provide subsurface measurements in conjunction with the airborne measurements. We also conducted airborne measurements and in situ measurements at the mouth of the Columbia River for one to two weeks each during July and September 2013.

Our approach benefits both the remote sensing research (by leveraging the RIVET in situ measurements) and RIVET itself via our integrated remote sensing and DA modeling system. The combined capabilities provide an innovative solution that couples spatially dense sampling with data assimilation methods to study the complicated dynamics of interacting wave, bathymetry, and current fields. The key to this project is an interactive process that blends sophisticated remote sensing, in-situ sensing, and data assimilation modeling. Our approach is to conduct closely coupled field and numerical model experiments to test the hypotheses listed above. Work on each facet informs the work on the others, and conflicts in results or interpretations are resolved by testing the hypotheses and the sensitivity of the results to a range of parameter variations.

WORK COMPLETED AND RESULTS

During the fifth year, worked on analysis and assimilation of the data from the pilot experiment at Duck, NC, RIVET I DRI experiment at New River Inlet, NC, and the RIVET II DRI experiment at the mouth of the Columbia River.

Due to the number of investigators involved and the complexity of the project, we have chosen to provide a section for each team which combines their Work Completed and Results contributions. The lettered sections correspond to the following teams:

A. Infrared Remote Sensing and Lidar– UW: Chickadel and Jessup
B. Electro-Optical Remote Sensing – OSU: Holman
C. Microwave Remote Sensing – UW: Farquharson
D. Microwave Remote Sensing – OSU: Haller
E. In situ Measurements – UW: Thomson
F. In situ Measurements – WHOI: Elgar and Raubenheimer
G. Numerical Modeling and Data Assimilation – OSU: Ozkan-Haller and Kurapov

A. INFRARED REMOTE SENSING AND LIDAR – UW: CHICKADEL AND JESSUP

Wave Dissipation

Built on the successfully validated technique to remotely estimate 1D (cross-shore) wave dissipation in the surf zone from thermal imaging (*Carini et al*., 2015), we are developing 2D wave energy dissipation method. Again, this method is based on the wave roller stress model of *Duncan* (1981, hereafter D81), which is parameterized on remote measurements of wave roller length, L_r. The transition from a 1D, cross-shore method to a 2D technique will allow for direct estimation of wave-by-wave breaking dissipation and resulting forcing from wave radiation stresses. The method begins with identification of the active breaking wave roller, using *Carini et al*. (2015). For each frame of the video an automated algorithm characterizes individual wave major and minor axes, orientation, and crest-perpendicular roller length. Figure A1 displays an example map showing the identified rollers (a) and their roller lengths (b) overlaid the corresponding IR image map.

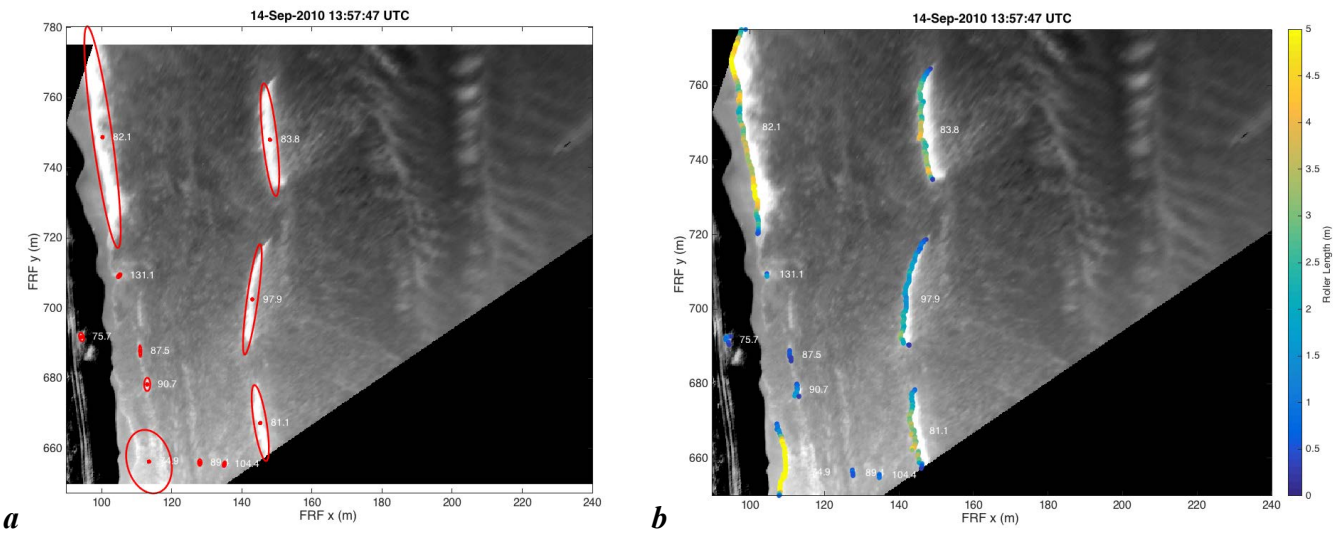

Figure A1. (a) Identified wave rollers approximated by an ellipse (red), and (b) wave-perpendicular wave roller length indicated by color plotted along each identified wave roller toe. The background is a rectified image from the IR camera, with the beach (dark, cool) on the left side of each panel. Note that the group of two small wave rollers in the bottom left of each image is misidentified as one larger roller.

Roller lengths and positions are used to then estimate the wave energy dissipation rates, ε_{D81}, using,

$$\epsilon_{\mathrm{D81}}(x,y,T) = \frac{1}{T}\sum_{t=1}^{T} 0.11\rho' g L_r^2(x,y)\sin(\alpha(x,y)) \tag{1}$$

where x and y are horizontal position, T is the time average length, ρ' is the roller density, and α is the wave face slope. The nature of the imagery data and the wave-by-wave estimates ε_{D81} from allow for exploration of the spatial and temporal variability of surfzone wave energy dissipation and forcing on many scales. For example choosing a typical wave-period time scale (10s) will approximate a wave-by-wave dissipation map, as shown in Figure A2. The true inhomogeneous nature of wave breaking and resulting energy dissipation is apparent in this example. Extension of this type of processing are planned to examining the spatial variability of wave breaking with different time scales from wave

average (seconds), to infragravity (100s) and tidal (hours). Combining wave direction estimates, also from the imagery, with dissipation rates we can produce radiation stress maps with unprecedented spatial and temporal resolution. These will eventual lead to capability to test theories of vorticity generation by individual waves (*Clark et al*., 2012), wave group forcing (Long and Özkan-Haller, 2009), and to directly feed surfzone circulation models.

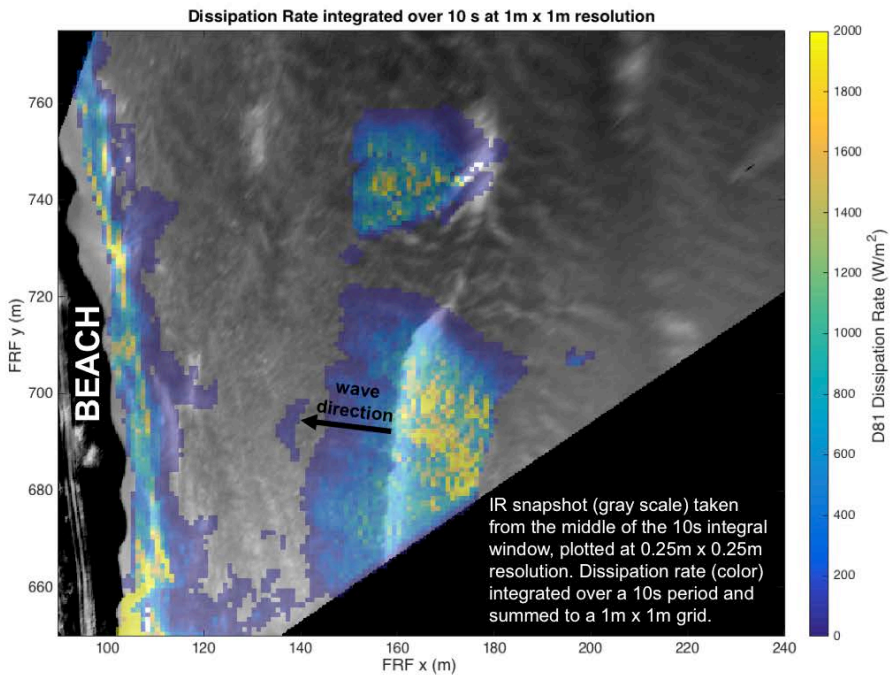

Figure A2. Wave-roller based dissipation estimates from the same time as show in Figure A1. The averaging time is 10s, and shows dissipation maps produced by individual breaking waves. Intermittent wave breaking over the bar (x = 160m) is more spatially varied than the wave breaking and energy dissipation at the beach (x = 110m).

Mouth of the Columbia River (MCR)

We have continued analysis of Remus AUV temperature, salinity and velocity data (Craig McNeil - APL), recorded simultaneously with the IR and ATI-SAR overpasses of the MCR internal hydraulic jump. We are focusing on obtaining estimates of the energy dissipation and mixing resulting from the jump and comparison with models. Our analysis is motivated by the significant role the internal jump could be playing in the estuarine and nearby coastal (plume) circulation, and by the unknown ability of circulation models to reproduce this feature. Because of the potential impact of tidally rectified mixing on the production rate of plume water, the depth of the plume, and estuarine circulation, the hydraulic jump may significantly affect residence time of waters within the estuary. This may impact the state of the estuary's ecosystem through altered phytoplankton residence time, nutrient, and oxygen fluxes (especially during upwelling periods). However, the total mixing resulting from the jump compared with other sources within the estuary and at the near-field plume lift off point at the mouth is not known. Analysis has been completed by F. Shi (UD) using the NHWAVE high-resolution numerical model (*Shi et al*., *in preparation*). The NHWAVE model is able to reproduce the internal structure of the jump and indicates dissipation of approximately 5 MW of energy per km of the internal jump length (the jump is approximately 3km long from remote sensing maps). Even considering the jump's intermittent nature, it can be expected to make a significant contribution to the total energy dissipation

within the interior of the Columbia River estuary, which is estimated to be 12–52 MW based on the modeling study of *MacCready et al*., [2009]. Any additional mixing by the downstream instabilities shown in the NHWAVE model and remote sensing data remains un-quantified.

We are also testing routinely used models for their applicability to produce the observed stratification and presence of the internal jump, using the composite Froude number *G* as a diagnostic. For continuously stratified flow, multiple vertical modes may exist, each with its own phase speed. Obtained dispersion relationship for long internal wave modes can be used to diagnose the onset of the hydraulic jump conditions. An example of this kind of analysis, shown in Figure A3, graphs the computed composite Froude number *G*, for the AUV data versus SELFE model data for the same time, which show agreement in shape and magnitude. However, the model output does not show a change from supercritical to subcritical or critical flow, as was seen in the data.

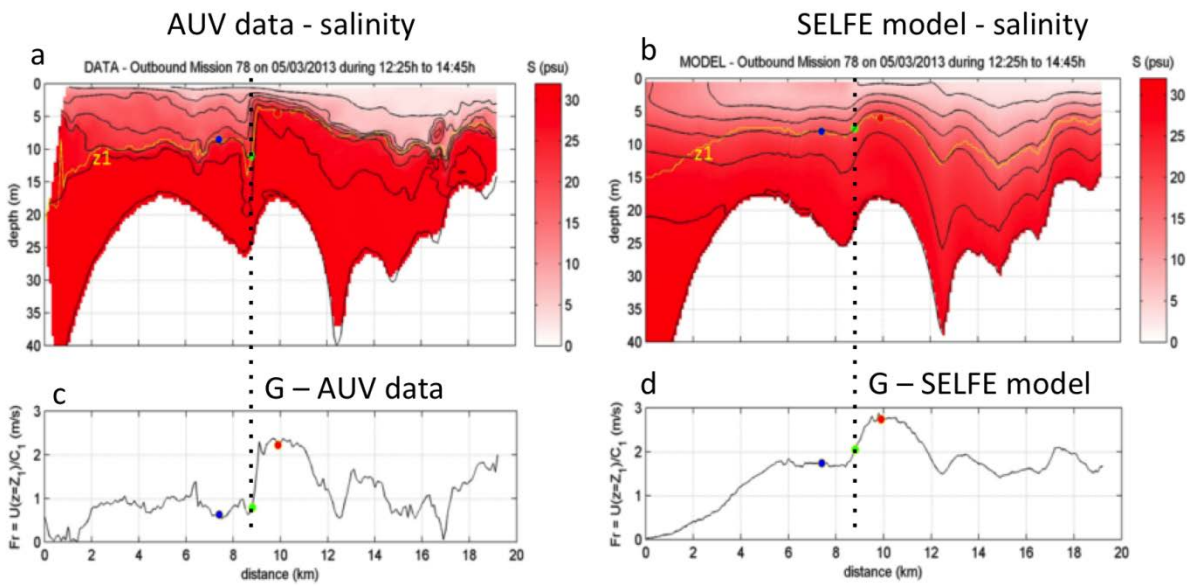

Figure A3. Observed (a) and SELFE modeled (b) salinity profiles from AUV transect through the internal jump. An internal wave mode was derived from the velocity and salinity structure in each to determine a conservative internal Froude (G) number for the velocity at the layer interface for (c) data and (d) model. Note agreement in shape, but disagreement in overall levels.

B. ELECTRO-OPTICAL REMOTE SENSING – OSU: HOLMAN

The goal of the electro-optical component of DARLA is to develop and test algorithms for estimating relevant geophysical variables based on electro-optical (EO) data, to work with modelers who will be developing methods to assimilate these data using appropriate statistical methods of data assimilation, and to compare data to synchronous results from companion radar and infrared sensors to search for new opportunities in data fusion. The work has been focused on three field experiments, the two-week Surf Zone Optics experiment at Duck, NC in September, 2010, a three-week field experiment in the unjettied New River Inlet in May, 2012 and a roughly five-week experiment at the Mouth of the Columbia River (MCR) in May-June, 2013. The electro-optical component of the Duck and MCR work has continued to the current time. Time series data from optical collections have been made

available on the standard Argus ftp site in MATLAB format and with readme's for all other investigators.

Our main effort over the recent years of the grant centered on cBathy, a robust method for bathymetry estimation based on time series of wave celerity and considerable signal processing [*Holman et al.*, 2013]. The algorithm has proved to be surprisingly robust under a variety of environmental conditions ranging from Pacific Swell to shorter North Sea waves. While the core cBathy capability is now operational, research continues on a number of aspects. The problem of solving for bathymetry in the presence of significant tidal currents was apparent in both of the RIVET experiments and is the subject of continuing research jointly with Drs. Haller and Honegger (in their case using radar data). We have developed a new algorithm for limiting dispersion sensitivity as depths move close to being hydrodynamically deep, an implementation that is now being tested. Work also continues on methods to merge shoreline data from other sources with cBathy, in recognition that cBathy shoreline estimates are unreliable.

Work continues on understanding the performance of nearshore numerical models whose inputs have been supplied solely from remote sensing data.

We also continue background efforts to transition Argus based optical remote sensing methods to small quadcopters, seeking to find the best conops including viewing angles and to understand dwell-limited cBathy performance.

Finally, we have continued work on understanding the physics and exploitability of internal ship wake data observed in wave-averaged movies.

Studies of the model use of remote sensing input data have yielded two papers. Wilson et al. [2014] explored the impact of different types of remote sensing data on bathymetry estimation using an ensemble Kalman filter approach to data assimilation. They found that remote sensing data assimilation significantly improved estimated bathymetry and circulation predictions. Rademacher et al [*Rademacher et al.*, 2014] carried out a similar study but based on an entirely different model (CoSMoS) and under a very different wave environment (North Sea), finding that rip currents systems could be reasonably estimated based solely on cBathy-derived bathymetry. This result has significant implications for swimmer safety predictions in The Netherlands.

Work that was previously in review has now been published on the morphology of the ebb delta at New River Inlet. Instead of a simple ebb delta morphology, Argus images collected a 23-day period during the RIVET I experiment showed that 66% of the variability occurred at meso-scale wavelengths (10-100 m) and migrated in a clear clockwise gyre with migration rates up to 3.5 m/day [*Pianca et al.*, in press].

Finally, a forty-year history of the evolution of nearshore processes research has been published [*Holman et al.*, 2015], a result of a nearshore community meeting to celebrate the forty-year career of Abby Sallenger and develop a vision for the best directions for future research. This and the companion future look paper have formed the basis for a reorganization of academia, government and industry to coordinate research efforts on major national problems.

C. MICROWAVE REMOTE SENSING – UW: FARQUHARSON

ATI-SAR Currents at the MCR

We updated our velocity field synthesis tool that merges velocity measurements from different aircraft passes into a single velocity field. The update eliminates the artificial discontinuities generated by the processing that were present in the previous versions of the velocity fields. We also upgraded the synthetic aperture radar (SAR) processing code to georeferenced SAR images more precisely in any geographic projection. This update allowed us to restructure the processing code to make it more computationally efficient for processing data over larger areas.

We have reprocessed the MCR ATI SAR data with the new processing code. The results of a merged velocity field synthesized from data collected between 20:39 and 21:26 UTC on June 10, 2013 is shown in Figures C1 and C2 (maximum flood was around 20:44 PDT). The wind was around 5 m/s from the west (259 degrees). A sharp change in flow direction from southwest to east-southeast is observed the area between the North Jetty and Jetty A (aka, the middle ground). This flow is indicative of water between the jetties being released from this area, and merging with the flood-driven flow. There is significant wave refraction and wave breaking visible west and northwest of Clatsop Spit. East of Clatsop Spit, the flow is southwest, in line with the direction of the main channel.

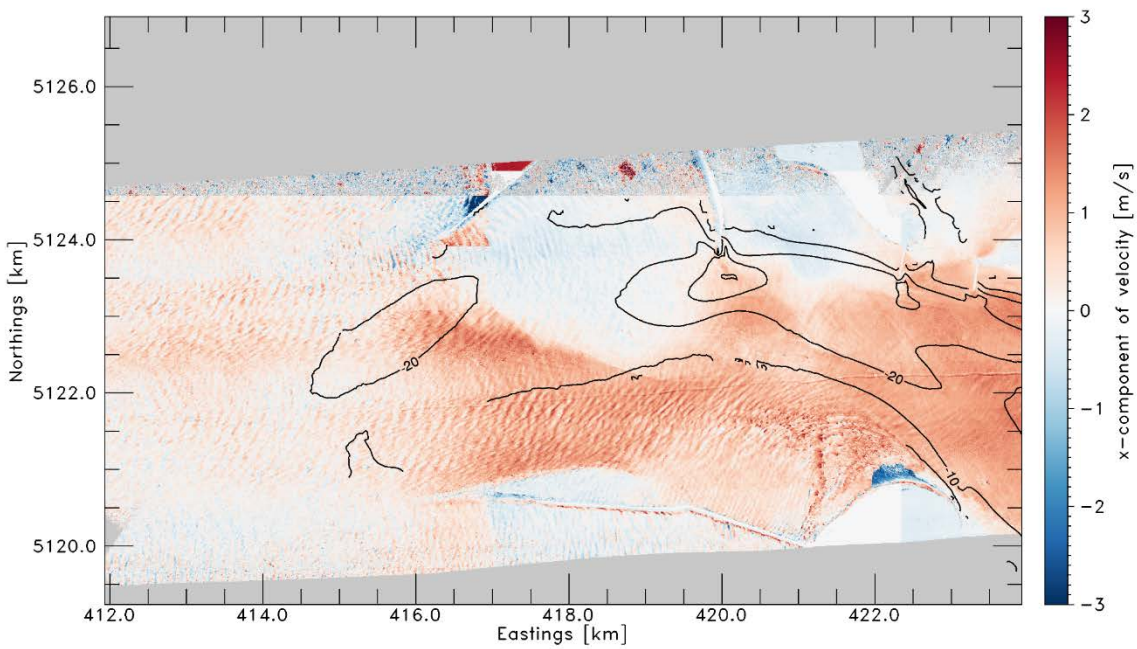

Figure C1: x-component of the surface velocity field measured by the radar. The image is a mosaic of data collected between 20:39 and 21:26 UTC on June 10, 2013. Maximum flood flow was predicted to occur at 20:44 UTC.

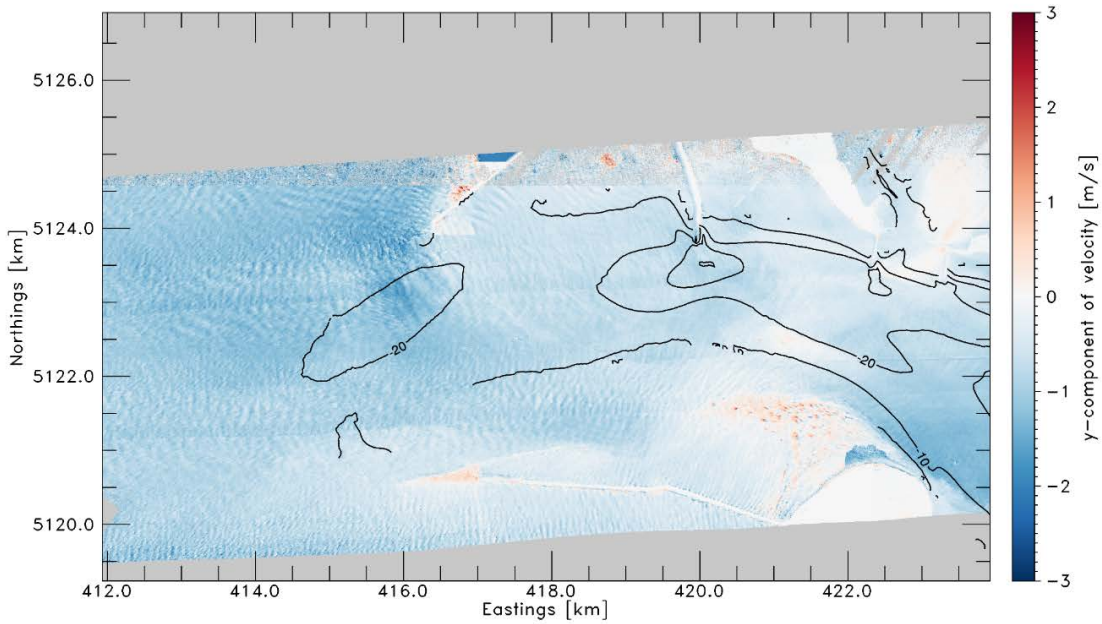

Figure C2: y- component of the surface velocity field measured by the radar during the same period as that shown in Figure C1.

Estimating Wave Parameters from ATI SAR

We extended our analysis of the MCR ATI-SAR data to study wave transformation in the mouth of the Columbia River. Wave length and direction were estimated from small (750 m by 750 m) areas in the mouth (Figure C3). We used a linear transformation developed by Bao et al. (1999) to convert spectra of ATI SAR interferograms to ocean wave spectra. We used NDBC buoy data from offshore of the mouth to initialize the transformation, and surveyed bathymetry data to convert wave length to wave period for comparison with the NDBC buoy measured wave period. Results from the data analyzed to date are shown in Figure C4. This work was presented at the 2015 IEEE International Geoscience and Remote Sensing Symposium. We are working to process more cases using this technique and to estimate error in the wave products.

Figure C3: Analysis regions in the mouth of the Columbia River for wave parameter estimation from ATI-SAR data.

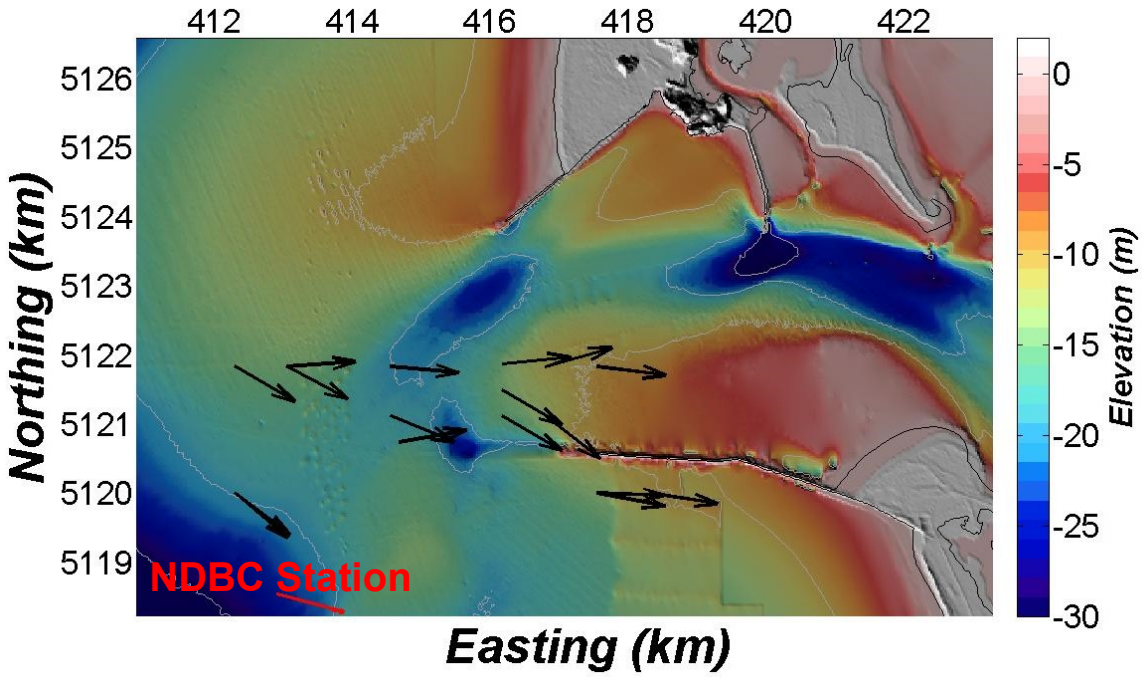

Figure C4:Wave direction (black vectors) in the mouth of the Columbia River estimated from ATI-SAR data collected on June 6, 2013. Mean wave direction at this time measured by NDBC buoy 46243 is indicated by the red vector. Bathymetry provided by Guy Gelfenbaum at the USGS.

Collaborations

ATI SAR data was provided to David Honegger to support his analysis of internal hydraulic jumps at the North Jetty and Jetty A (manuscript in preparation). ATI SAR data was also provided to David Walker of SRI, for data assimilative modeling at the MCR.

D. MICROWAVE REMOTE SENSING – OSU: HALLER

We have completed development of a methodology to rapidly assesses wave transformation through a tidal inlet using wave imaging radar time series. The method utilizes radar-derived estimates of wave breaking frequency, wave dissipation and bathymetry to drive an inverse model of the 1-D cross-shore energy flux model. Estimated wave heights using this method were compared against those observed during a 9-day period, resulting in correlation values R = 0.68 to 0.96 and RMS errors 0.05 to 0.19 m. Wave forcing due to radiation stress gradients was also computed and cross-shore forcing was onshore during high-wave conditions, in good agreement (R = 0.95) with observations (Figure D1). This work was published in the *Journal of Atmospheric and Oceanic Technology* (*Díaz-Mendez et al.*, 2015).

We also performed extended analyses of radar-derived depth and current estimation capabilities. Simultaneous inversion of both depth and the mean current vector is attractive, but the often narrow directional spread of the wave field hampers estimates of the full current vector. At the relatively high spatial resolution of the cBathy algorithm (*Holman et al., 2013*), this limitation can result in poorly constrained depth estimates. Utilizing the long dwell advantage of shore-based remote sensing platforms, one may temporally average depth-only estimates at a tidal inlet through multiple tidal cycles to mitigate the effect of the oscillating currents. Despite the nonlinear effect of this Doppler shift on the depth estimates, this method was found to be surprisingly effective at a shallow inlet with

moderate current magnitudes. Figure D2 shows contours of the resulting fractional error in estimated depth when currents are neglected; Figures D2a and D2b compare the histograms of observed conditions at the Mouth of the Columbia River (MCR) and at New River Inlet (NRI). In-situ data were provided by Guy Gelfenbaum (USGS), and Steve and Britt Raubenheimer (WHOI) for the two sites, respectively. The conditions observed at New River Inlet lie within a linear region (bounded by the dashed line), in which tidal averaging produces negligible bias. This analysis was presented at the AGU Fall Meeting in 2014 and the tidal averaging method was used to produce depth estimates at NRI in *Díaz-Mendez et al.* (2015).

More detailed analyses of internal bore models were completed in the context of the oblique, internal hydraulic jumps first observed in 2013 at the MCR. We extended our understanding of the hydraulic feature beyond the 1.5-layer model, in which one layer is assumed inactive throughout, to a fully 2-layer model, in which the internal jump amplitude can be limited. The latter class of model better characterizes the conditions surrounding the internal jumps at the MCR. Despite discussion in the literature regarding where in the water column energy is preferentially dissipated (e.g., *Yih and Guha*, 1955, *Klemp et al.*, 1997, *White and Helfrich*, 2014), the conjugate-state bore is a common large-amplitude limit (*Lamb, 2000*). The small-amplitude, linear bore model and the conjugate-state bore model can then be used to place bounds on the estimated angle of the oblique, internal jumps in the presence of observed upstream velocity and density profiles. These analyses were implemented in revisions of *Honegger et al.* (2014).

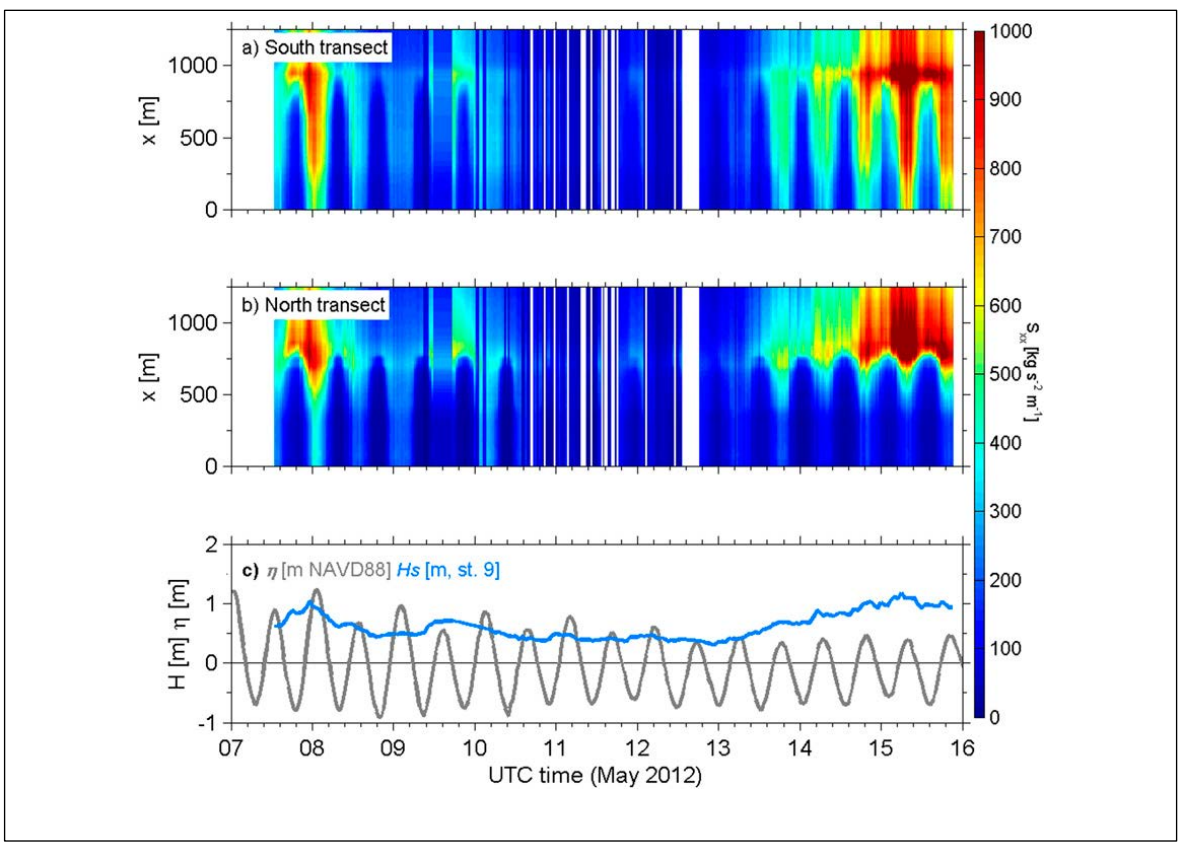

Figure D1: Predicted cross-shore radiation stress, S_{xx}, (color contours, scale on the right) as a function of cross-shore location and time for the (a) north and (b) south channels. (c) Observed offshore significant wave height (blue curve) and tidal elevation (gray curve) vs time.

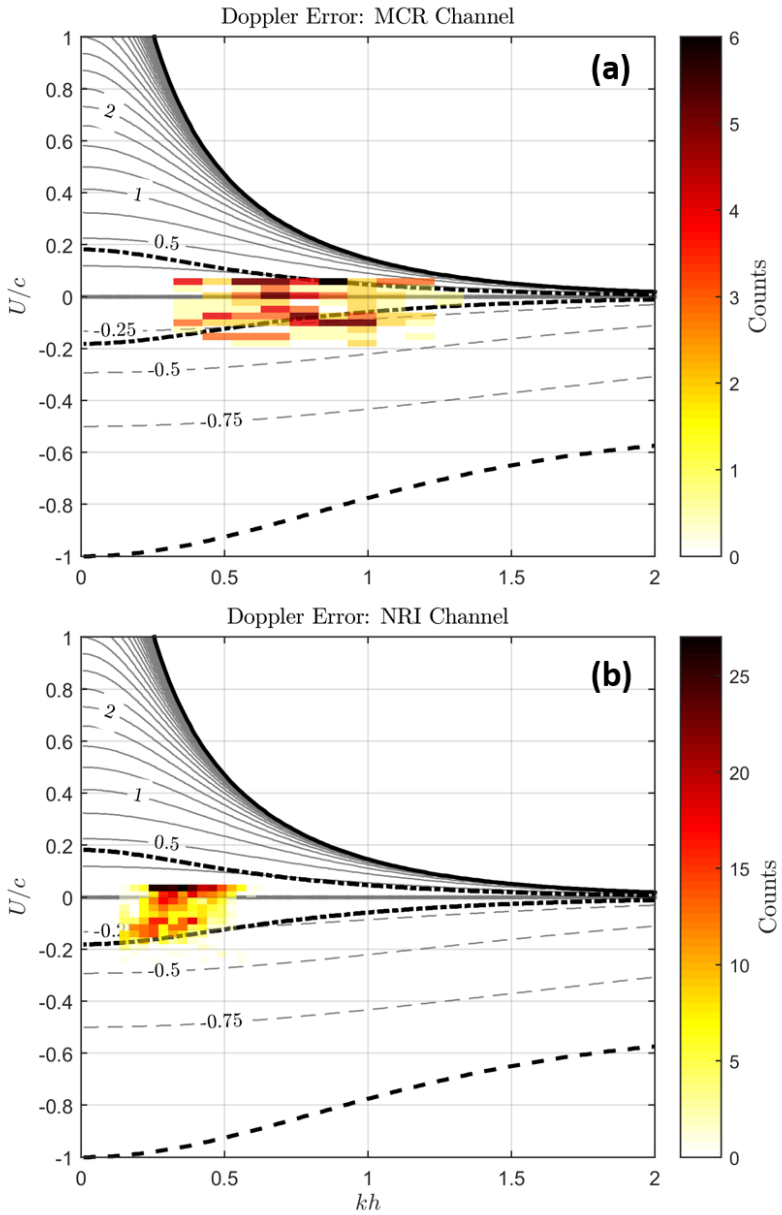

Figure D2: Fractional depth estimate error (Δh/h) incurred by neglecting the Doppler shift of currents, as a function of relative depth (kh) and nondimensional current speed (U/c). Following currents result in depth over-estimates (solid contours) and counter-currents result in under-estimates (dashed contours); a near-linear region near the zero contour is bounded by a thick, dashed line. (a) Observed conditions at the Columbia River Mouth, OR/WA; (b) observed conditions at New River Inlet, NC.

E. IN SITU MEASUREMENTS – UW: THOMSON

In FY15, the primary work has been analysis of data collected from Surface Wave Instrument Floats with Tracking (SWIFTs) at the Mouth of the Columbia River in 2013. The quality controlled data are now publically available at http://faculty.washington.edu/jmt3rd/SWIFTdata/ColumbiaRiverMouth/. Although most of the data was processed and availble imediately after the experiment, the processing

of onboard video data to obtain the breaking fraction, Q_b, of the waves has been a significant additional effort. This began in FY14 and has continued into FY15. This processing is semi-automated, such that a scoring algorithm flags image frames with a high likelihood of containing a breaking wave and these images are then manually reviewed. This method has been published in a conference proceeding (Rusch et al, 2014). The breaking fraction is preferred over the breaking rate, because this rigorously accounts for the moving reference frame of the SWIFTs in a normalization of the breaker count by the number of waves observed. Figure E1 shows an example of the breaking fraction Q_b calculated for two sequential days of drift deployments. Both days show wave breaking (high Q_b) at the 'bar' (longitude = -124.0), but only one of the two days has wave breaking at the offshore front formed by the river plume expanding into the ambient salt water (longitude = -124.3).

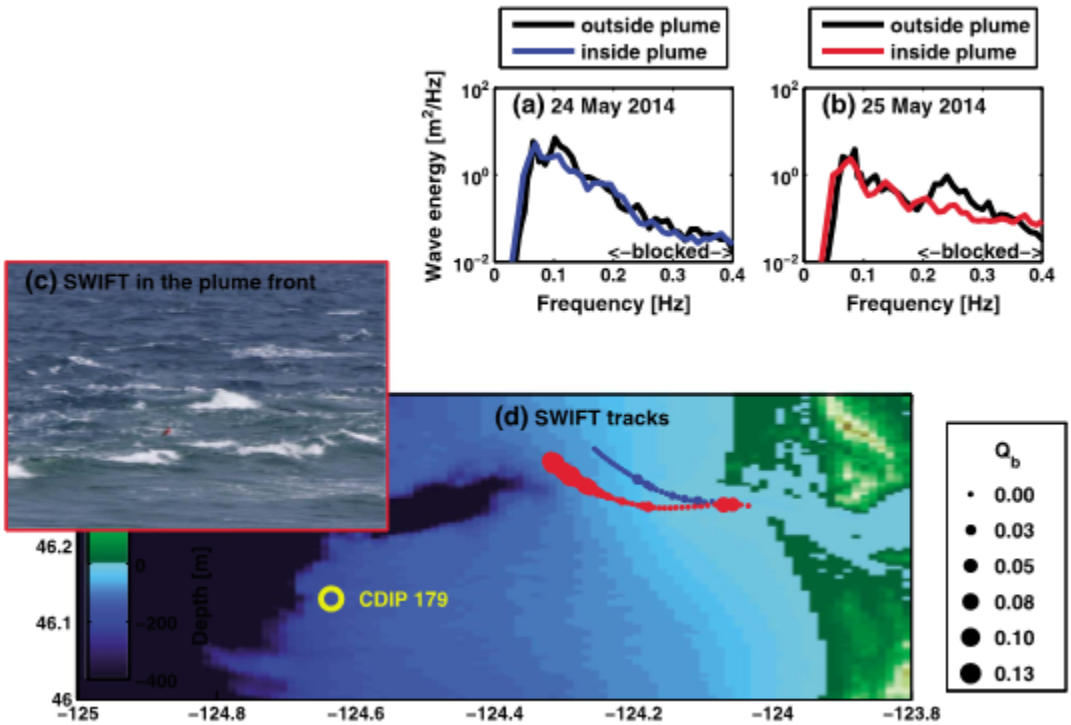

Figure E1. Wave spectra and SWIFT drifter tracks from 24 and 25 May 2013 at the Mouth of the Columbia River. The symbol size for the drifter positions is scaled by the breaking fraction, Q_b, and shows enhance breaking over the 'bar' for both days. Only the 25th, however, has enhanced breaking offshore, where the river plume creates a sharp front and blocks an onshore directed wind sea that occurred on that day. (From Thomson et al, 2014.)

There are two primary results from SWIFT data analysis completed in FY15. First, we have shown that short waves breaking at the offshore front of the Columbia River plume can provide a significant amount of tuburblent kinetic energy (TKE) that may enhance the mixing of salt and fresh water. This is demonstrated by contrasting two sequential days in May 2013. Both days have similar ebb tide velocities and river discharge, but one day (25 May) has a wind sea that breaks at the front between the fresh and salt water. A strong onshore wind generated these waves and they break when they encounter the gradient in current from ambient salt water (0 m/s) to the expanding plume (2 m/s).

Figure E2 shows the near-surface profiles of the TKE dissipation rate at the plume front on these days, and extrapolates these values downward to the base of the plume.

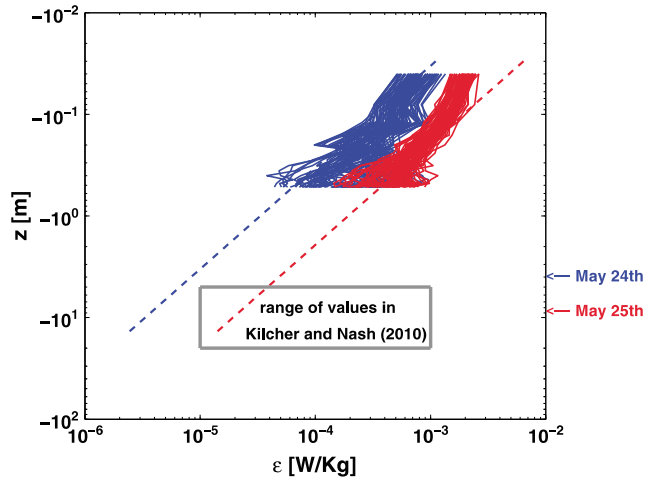

Figure E2. Vertical profiles of Turbulent Kinetic Energy dissipation rate from 24 and 25 May 2013 at the Mouth of the Columbia River. Dashed lines extrapolate these profiles downward to the interfacial depth and a box shows the range of published values for interfacial turbulence in this region. On 25 May, the enhance of turbulence associated with wave breaking is sufficient to alter the existing turbulence.

The second primary result is the diagnosis of the wave breaking itself, which uses a spectral steepness parameter. This extends earlier work in this project from the New River Inlet site, which was just published as Zippel & Thomson (2015) and incorporated current effects in depth-limited breaking. In the new results, a spectral steepness approach incoporates currect effects for breaking from deep to shallow water. This universal approach sets a steepness limit for each wavenumber, which can be related to absolute frequency using a dispersion relation that includes current. The advantages of this approach are most evident at a site such as the MCR, where the currents are strong and the depths are large relative to wave heights. Figure E3 shows an example of this method. The example indicates that below long and short waves are likely to be breaking, and this is confirmed by the onboard video processing.

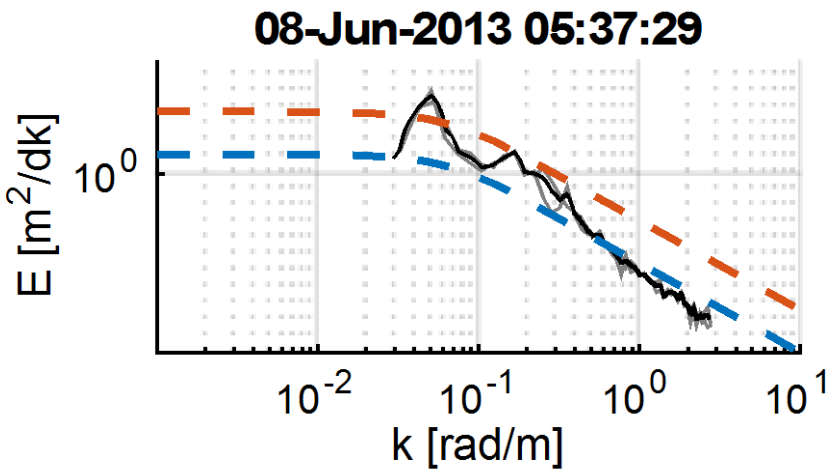

Figure E3. Observed wave spectrum (black line) and spectral steepness limits (dashed lines). This example has long waves that exceed the shallow-water steepness limit (orange dashed line) and short waves that are just equal to the deep-water steepness limit (blue dashed line).

F. IN SITU MEASUREMENTS – WHOI: ELGAR AND RAUBENHEIMER

Observations from wave and current sensors deployed at 32 locations near New River Inlet from April 27 through June 1, 2012 are being used to initialize, test, and improve numerical models for waves and currents (Figure F1) and as ground truth for remote sensing studies.

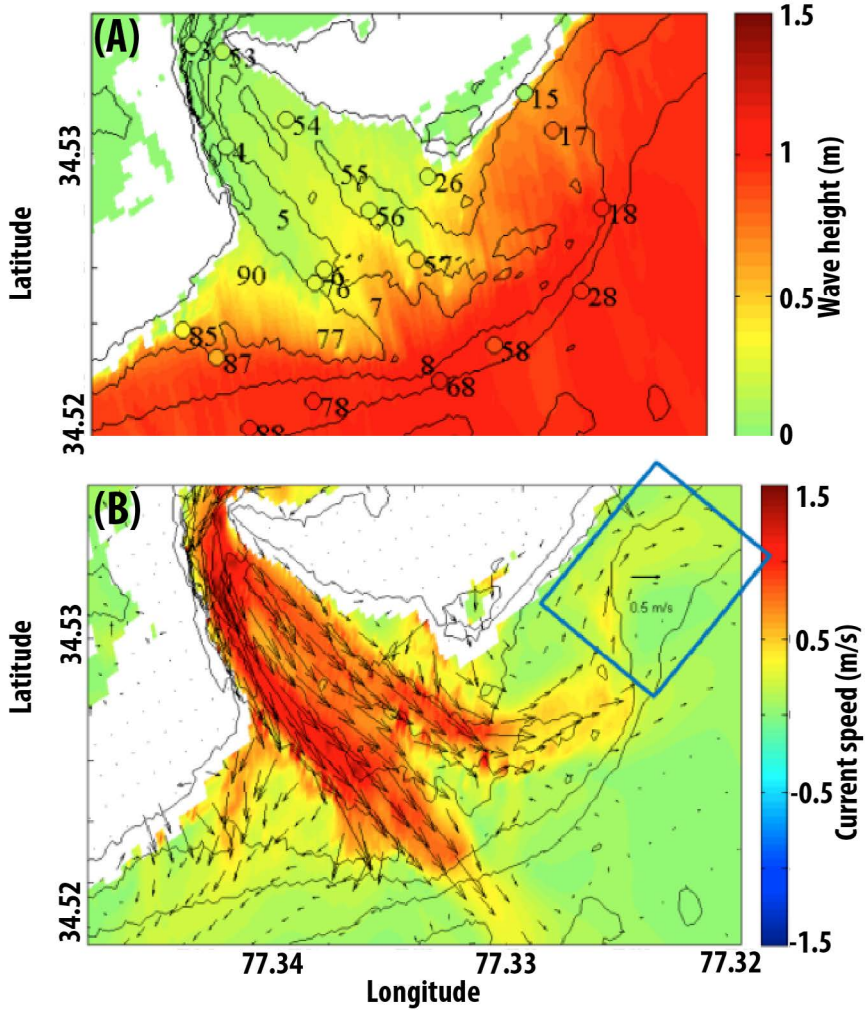

Figure F1. (A) Modeled (color contours) and observed (colors inside the small circles at numbered sensor locations) wave heights during maximum ebb at New River Inlet on May 27, 2012, a spring tide-stormy wave condition. If model and data agree, the color inside the circle matches the color of the surrounding model contours. (B) The modeled instantaneous flow field (vectors indicate direction and color contours indicate current speed, scale on the right) during maximum ebb on May 27th. The solid curves are bathymetric contours (0, 2, 4, 6, and 8 m depth relative to NAVD88). [The model predicts the observed waves accurately and simulates the complex inlet and nearshore flows.]

The NEARComm nearshore circulation model coupled with the SWAN wave model predicts the observed wave heights accurately (Figure F1A). The model also predicts the currents accurately (not shown, see Chen et al. 2015).

G. NUMERICAL MODELING AND DATA ASSIMILATION – OSU: OZKAN-HALLER AND KURAPOV

Numerical modeling work has progressed on multiple fronts. At New River Inlet (NRI), we have refined our bathymetry estimation methodology and have been exploring uncertainty estimates on the results that can be of practical benefit. We have also been further exploring the utilization wave model results along with SWIFT drifter data to assess the vertical distribution of wave breaking turbulence and the connection of the sub-surface signature to surface quantities. Finally, we began simulating the temperature and salinity fields at NRI in anticipation of comparisons with observations of frontal features. At the Mouth of the Columbia River (MCR), we have continued data-model comparisons with lidar-based wave height observations as well as begun comparisons with radar-derived frontal features. Below the results of these efforts are discussed in more detail.

Our modeling methodology is based on a coupled circulation and wave modeling system (ROMS+SWAN using COAWST) and an ensemble-based data assimilation approach. We had previously tested our methodology using "synthetic" (model-derived) observations. We have since refined the approach and applied it at NRI using observations from multiple sources. In particular, observations of surface currents from SAR imagery, wavenumber estimates from X-band radar observations and flow speed estimates from SWIFT drifters are utilized. The first-guess (prior) bathymetry consists of a generic smooth channel and water depths that increase monotonically towards the ocean. The resulting bathymetry estimate is an improvement over the prior first-guess bathymetry and includes more accurate estimates of the two distinct channels in the inlet along with the shoals around them (see 2014 report). In addition to the updated bathymetry estimate, the data assimilation methodology also produces an update on the covariance estimates. These are interpreted as indicative of the uncertainties in the produced bathymetry estimate and give an indication of the how much confidence the method itself has in the bathymetry estimate it has produced at a given location. As an example, the uncertainty estimates associated with several assimilation experiments are given in Figure G1. The uncertainty associated with the prior (which is user-specified) is high and uniform over most of the domain (panel a). The simulations assimilating only circulation observations (from SAR or SWIFT observations in panels b and c, respectively) show reduction of uncertainties where data is available and currents are strong. Outside of the inlet mouth the uncertainty estimates revert back to the prior uncertainty. Essentially the method is indicating that bathymetry estimates in areas where no reduction in uncertainty has been attained should be interpreted as equivalent in quality to the prior estimate. Hence, not surprisingly, the uncertainty estimates involving only wave observations (which cover an area at and outside the inlet mouth) indicate that the bathymetry is improved outside of the inlet mouth but not up the river. When all measurement types are used, uncertainties are reduced over the majority of the domain. Hence, the uncertainty estimates produced by the method provide a way to assess the bathymetry estimates in the absence of any ground truth. These results are now included in a recently resubmitted publication.

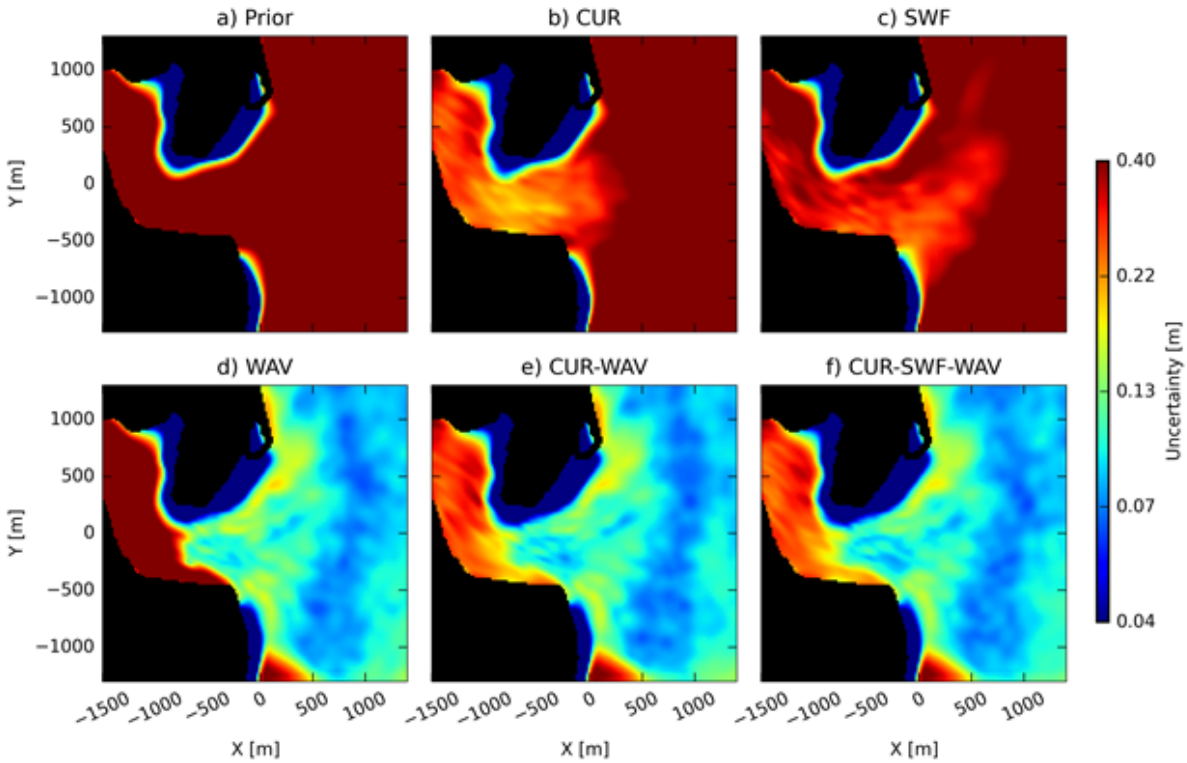

Figure G1: Uncertainty estimates associated with (a) the prior bathymetry and bathymetry estimates assimilating (b)SAR surface current observations, (c) SWIFT drifter observations, (d) radar-derived wave observations, (e) both wave and current observations, and (f) all available observations. Reduction in the posterior uncertainty estimates (over the prior) indicates areas where the method has confidence that the posterior bathymetry estimate is an improvement over the prior.

Another area of inquiry at NRI has been centered around estimating water column turbulence quantities. For this purpose, the coupled wave-circulation modeling system was further coupled with a vertical turbulence model that considers the injection of turbulence due to wave breaking events. For cases involving wind speeds in excess of 6 m/s and in water depths larger than 4m (to exclude depth-induced breaking events), data-model comparisons neglecting wave breaking turbulence indicated an under-prediction of water column turbulence dissipation rate by several orders of magnitude. Inclusion of turbulence injection due to wave breaking markedly improved estimates (see Figure G2 for data-model comparisons of the turbulent dissipation rate for 6 example drifters). A publication detailing these findings (along with further analysis) is now in re-review.

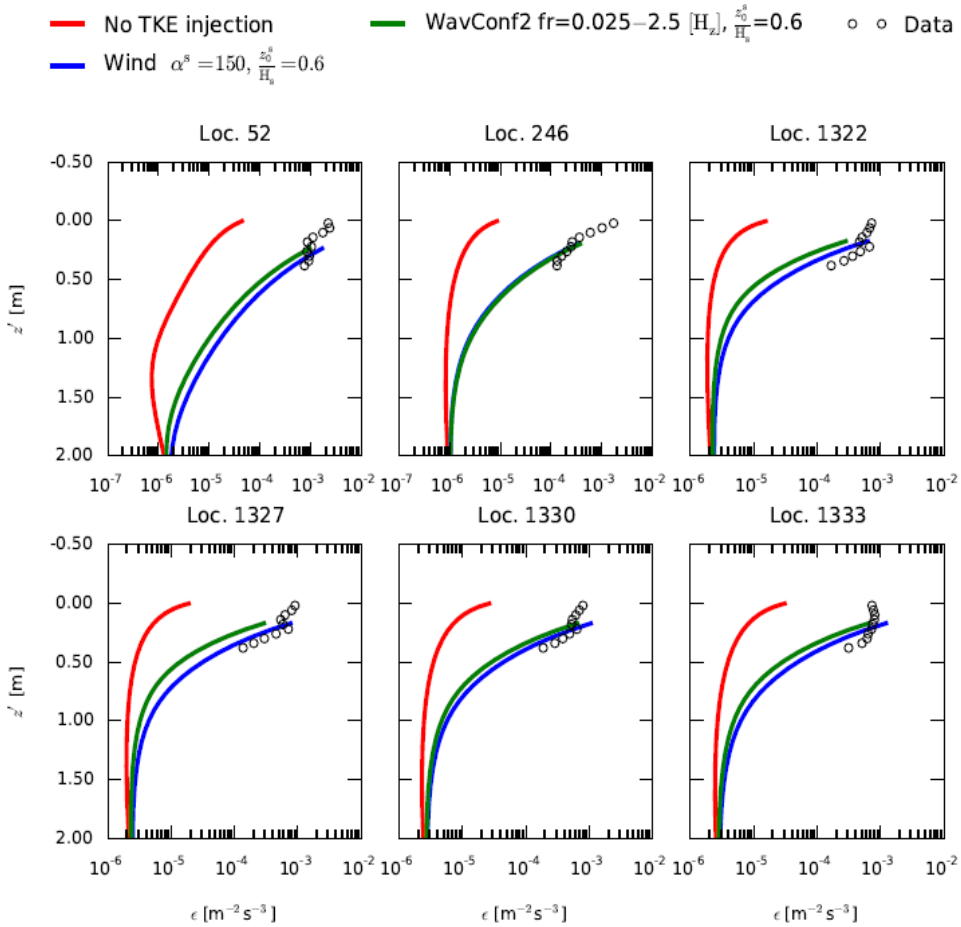

Figure G1:Depth versus turbulent dissipation rates for 6 SWIFT drifters compared with model results excluding wave breaking effects (red) and including wave breaking effects with two different parameterizations (green and blue). The simulation neglecting wave effects under-predicts the dissipation rate by several orders of magnitude, whereas the simulations including wave effects show much improved performance.

Modeling efforts at the MCR involve coupled model runs for realistic conditions. The specific modeling setup used herein is nested into a larger scale coastal circulation model with a domain that encompasses the entire Oregon continental shelf. This outer model predicts the occurrence of upwelling/downwelling events and provides an accurate representation of tidal currents and river discharge. The MCR model simulations account for coupling between the wave and circulation fields. We have carried out comparisons with a variety of data types. Most recently, we have analyzed data-model comparisons with novel lidar-derived wave height estimates (see Figure G3). We find favorable agreement with the observations (RMSE=0.54m for wave heights reaching 3.5m and a skill value of 0.86) both inside and outside the inlet mouth.

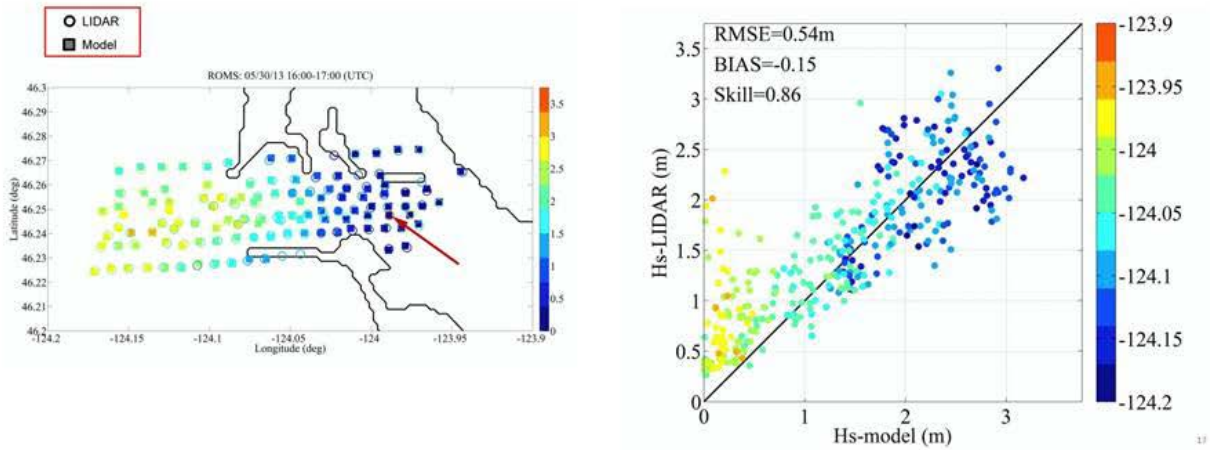

Figure G3: Data-Model comparisons with lidar-derived wave height observations at the Mouth of the Columbia River. (a)Observations (color circles) and model results (filled squares) over the domain (with warmer colors representing larger wave heights) indicating larger offshore wave heights and a sharp transition to lower wave heights inside the estuary that is reproduced by the model results, (b) scatter plot of observed wave heights versus modeled wave heights (warmer colors indicating lower latitudes) with error estimates of RMSE-0.54m, BIAS=0.15m and model skill value of 0.86.

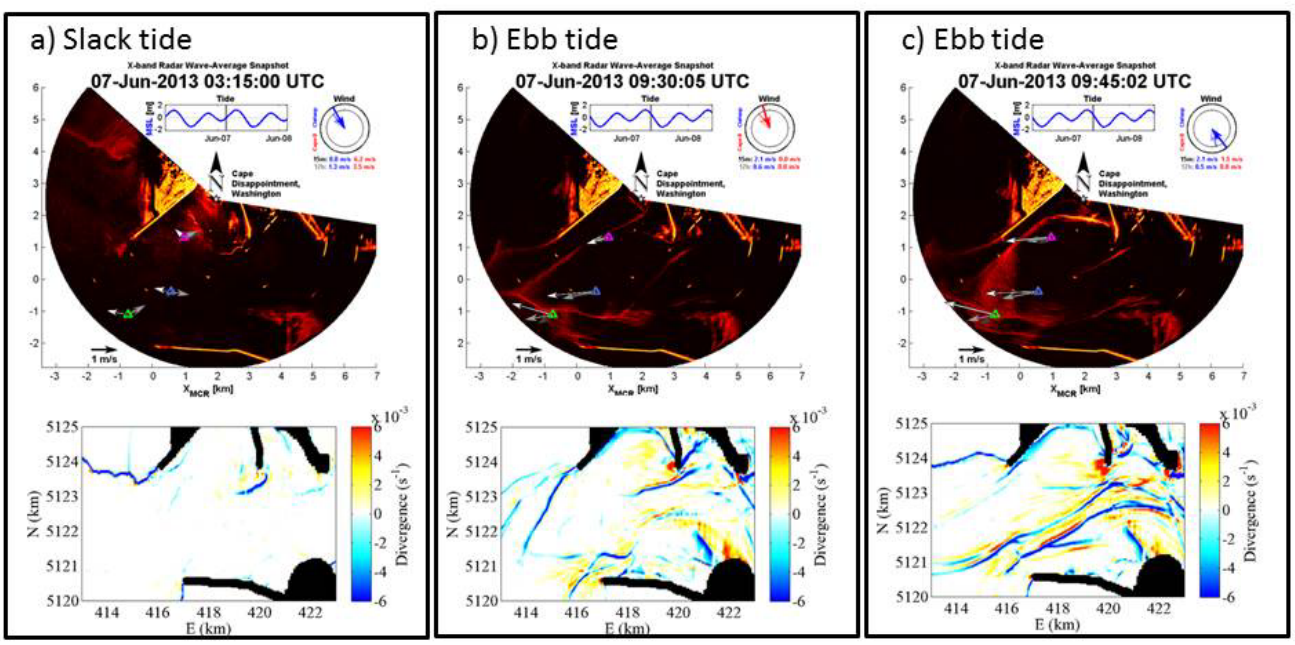

Figure G4: Observed convergence features from radar images (top panels) and divergence estimates from model results (bottom panels) for (a) a slack condition, (b) an ebb condition, (c) later in the tidal cycle for the ebb condition. Features resenbling convergence lines in the model results are also seen in the radar images.

Finally, we have been intrigued by the frontal features revealed by the wave-averaged radar images. Building on the hypothesis that bright features in these images correspond to surface flow convergences, we have computed surface convergence/divergence fields using 3D simulations at both sites. Here, we will discuss such estimates for the MCR (see Figure G4). We find that convergences seen in the model results qualitatively resemble the observations. For example, a convergent feature at the tip of Jetty A during slack tide is also seen in the obserbations (panel a). A convergence line at near the tip of the north jetty during ebb tide that is intersected at an angle by another, albeit weaker, convergence line is also visible in the observations (panel b), though at a somewhat different position. Finally, a convergence feature that is nestled in the corner between Jetty A and the north jetty is also seen in the observations (panel c). Whether or not the resemblances in the modeled and observed fronts can be leveraged to gain a better understanding of the subsurface dynamics (including the underlying bathymetry) remains to be explored.

IMPACT/APPLICATIONS

Our results demonstrate how currently available prediction schemes and remote sensing observing systems can be combined for operational applications. Use of a miniaturized airborne along-track-interferometic SAR to measure surface velocities provides a new and powerful tool for area-extensive measurements in the field. The development and successful testing of cBathy under a wide range of wave conditions and beach slopes has been a game changer for nearshore remote sensing. Similar results are seen using cBathy on marine radar data.

RELATED PROJECTS

Inner Shelf DRI
Our routine remote sensing sampling and analysis are currently in use for the ONR Inner Shelf DRI. We completed a pilot experiment off the coast of central California in which we observed fronts, internal waves and strong mixing signatures in the surface ocean.

This work complements the traditional interests of NRL-SSC in littoral remote sensing including efforts to carry out nearshore prediction based on UAV sensor inputs and all other remote sensing resources. This work is of very great interest in The Netherlands where many students and several large programs study and exploit nearshore remote sensing approaches.

The WHOI *in situ* wave and current observations near New River Inlet were collected as part of a DRI, and are being used to develop, test, and improve models for wave propagation, circulation, and morphological evolution, as well as to ground truth remote sensing observations.

The results from the wave breaking turbulence at the Columbia river plume front (Thomson et al, GRL, 2014) were used to motivate and guide a successful NSF proposal. The new project has just started and will extend the results from the Columbia to much smaller river plume systems, where the effects of wave breaking may be even more important because the interface of fresh and salt water is shallower in these systems.

REFERENCES

Díaz Méndez, G., M.C. Haller, B. Raubenheimer, S. Elgar, and D. Honegger, Radar remote sensing estimates of waves and wave forcing at a tidal inlet, *J. Atmos. Ocean. Tech.*, 32(4), pp. 842-854, 2015.

Bao, M., W. Alpers and C. Brüning (1999), A new nonlinear integral transform relating ocean wave spectra to phase image spectra of an along-track interferometric synthetic aperture radar, *IEEE Trans. Geosci and Remote Sensing*, 37(C1), 461–466, doi: 10.1109/36.739088.

Chen, J., T. Hsu, F. Shi, B. Raubenheimer, and Steve Elgar, Hydrodynamic and sediment transport modeling of New River Inlet (NC) under the interaction of tides and waves, *J. Geophysical Research,* **120***,* 4028-4047*,* doi:10.1002/2014JC010425.

Clark, D. B.*,* S. Elgar*, and* B. Raubenheimer *(*2012*),* Vorticity generation by short-crested wave breaking*, Geophys. Res. Lett., 39,* L24604, doi:*10.1029/2012GL054034*.

Holman, R.A., Plant, N., and T. Holland, cBathy: A robust algorithm for estimating nearshore bathymetry, *J. Geophys. Res.*, 118, doi:10.1002/jgrc.20199, pp. 2595-2609, 2013.

Honegger, D.A., M.C. Haller, and R.A. Holman, Bathymetry estimates on open beaches and in tidal inlets via remote sensing, Presented at the Fall Meeting (AGU), San Francisco, CA, 2014.

Klemp, J. B., Rotunno, R., & Skamarock, W. C., On the propagation of internal bores, *J. Fluid Mech.*, 331, pp. 81-106, 1997.

Lamb, K. G., Conjugate flows for a three-layer fluid. *Phys. of Fluids*, 12(9), pp. 2169-2185, 2000.

Long, J. W., and H. T. Özkan-Haller (2009), Low-frequency characteristics of wave group–forced vortices*, J. Geophys. Res.,* 114, C08004, doi:10.1029/2008JC004894.

MacCready P, N. Banas, B. Hickey, E. Dever, Y. Liu (2009). A model study of tide- and wind-induced mixing in the Columbia River estuary and plume. *Cont. Shelf. Res.*, 29 (1), 278–91.

White, B. L., & Helfrich, K. R., A model for internal bores in continuous stratification, *J. Fluid Mech.*, 761, pp. 282-304, 2014.

Yih, C.S. and C.R. Guha, Hydraulic jump in a fluid system of two layers, *Tellus*, 7(3), pp. 358-366.

PUBLICATIONS

1. Aslebash, S., and G. Farquharson (2015), Wave period and direction estimation in shallow water using airborne along-track interferometric synthetic aperture radar, paper presented at IEEE Geosci. Remote Sens. Symp. 2015, Milan. [published]
2. Carini, R., C. Chickadel, A. Jessup, and J. Thomson (2015), Estimating wave energy dissipation in the surf zone using thermal infrared imagery, *J. Geophy. Res.*, *120*, doi:10.1002/2014JC010561. [published, refereed]
3. Catalan, P. A., M. C. Haller, and W. J. Plant (2014), Microwave backscattering from surf zone waves, *J. Geophys. Res.-Oceans*, *119*(5), 3098-3120. [published, refereed]
4. Chen, J.-L., et al. (2015), Hydrodynamic and sediment transport modeling of New River Inlet (NC) under the interaction of tides and waves, *J. Geophys. Res.-Oceans*, *120*(6), 4028-4047. [published, refereed]

5. Diaz Mendez, G. M., et al. (2015), Radar Remote Sensing Estimates of Waves and Wave Forcing at a Tidal Inlet, *Journal of Atmospheric and Oceanic Technology*, *32*(4), 842-854. [published, refereed]

6. Farquharson, G., H. Deng, Y. Goncharenko, and J. Mower (2014), Measurements of the nearshore ocean with FMCW ATI SAR, paper presented at 10th European Conference on Synthetic Aperture Radar, Berlin, Germany. [published]

7. Goncharenko, Y. V., et al. (2015), Estimation of Shallow-Water Breaking-Wave Height From Synthetic Ap[published, refereed]

8. Holman, R., N. Plant, and T. Holland (2013), cBathy: A robust algorithm for estimating nearshore bathymetry, *J. Geophys. Res.-Oceans*, *118*(5), 2595-2609. [published, refereed]

9. Holman, R., et al. (2015), Advances in nearshore processes research: four decades of progress, *Shore and Beach*, *83*(1), 39-52. [published, refereed]

10. Kurapov, A. L., and H. T. Oezkan-Haller (2013), Bathymetry correction using an adjoint component of a coupled nearshore wave-circulation model: Tests with synthetic velocity data, *J. Geophys. Res.-Oceans*, *118*(9), 4673-4688. [published, refereed]

11. MacMahan, J., et al. (2014), Fortnightly tides and subtidal motions in a choked inlet, *Estuarine Coastal and Shelf Science*, *150*, 325-331. [published, refereed]

12. Moghimi, S., H. Ozkan-Haller, G. Wilson, and A. Kurapov (in review-a), Data assimilation for bathymetry estimation at a tidal inlet, *, J. of Atmos. And Oceanic Tech*. [refereed]

13. Moghimi, S., et al. (in review-b), On the modeling of wave-enhanced turbulence nearshore, *Ocean Modeling*. [refereed]

14. Moulton, M., S. Elgar, and B. Raubenheimer (2014a), A surfzone morphological diffusivity estimated from the evolution of excavated holes, *Geophysical Research Letters*, *41*(13), 4628-4636. [published, refereed]

15. Moulton, M., S. Elgar, and B. Raubenheimer (2014b), Improving the time resolution of surfzone bathymetry using in situ altimeters, *Ocean Dynamics*, *64*(5), 755-770. [published, refereed]

16. Orescanin, M., B. Raubenheimer, and S. Elgar (2014), Observations of wave effects on inlet circulation, *Continental Shelf Research*, *82*, 37-42. [published, refereed]

17. Pianca, C., R. Holman, and E. Siegle (2014), Mobility of meso-scale morphology on a microtidal ebb delta measured using remote sensing, *Marine Geology*, *357*, 334-343. [published, refereed]

18. Pianca, C., R. Holman, and E. Siegle (2015), Shoreline variability from days to decades: Results of long-term video imaging, *J. Geophys. Res.-Oceans*, *120*(3), 2159-2178. [published, refereed]

19. Radermacher, M., M. Wengrove, J. v. T. d. Vries, and R. Holman (2014), Applicability of video-derived bathymetry estimates to nearshore current model predictions, *Journal of Coastal Research*, 290-295. [published, refereed]

20. Rusch, C., J. Thomson, S. Zippel, and M. Schendeman (2014), Video recognition of breaking waves, paper presented at Oceans 2014, St. Johns, Newfoundland. [published]

21. Spydell, M. S., et al. (2015), Observed and modeled drifters at a tidal inlet, *J. Geophys. Res.-Oceans*, *120*(7), 4825-4844. [published, refereed]

22. Suanda, S. H., J. A. Barth, R. A. Holman, and J. Stanley (2014), Shore-Based Video Observations of Nonlinear Internal Waves across the Inner Shelf, *Journal of Atmospheric and Oceanic Technology*, *31*(3), 714-728. [published, refereed]

23. Thomson, J., et al. (2014), Wave breaking turbulence at the offshore front of the Columbia River Plume, *Geophysical Research Letters*, *41*(24), 8987-8993. [published, refereed]

24. Wargula, A., B. Raubenheimer, and S. Elgar (2014), Wave-driven along-channel subtidal flows in a well-mixed ocean inlet, *J. Geophys. Res.-Oceans*, *119*(5), 2987-3001. [published, refereed]

25. Wilson, G. W., et al. (2014), Surf zone bathymetry and circulation predictions via data assimilation of remote sensing observations, *J. Geophys. Res.-Oceans*, *119*(3), 1993-2016. [published, refereed]

26. Zippel, S., and J. Thomson (2015), Wave breaking and turbulence at a tidal inlet, *J. Geophys. Res.-Oceans*, *120*(2), 1016-1031. [published, refereed]